Effect of Corrugation Depth on Heat Transfer Enhancement and Flow Characteristics for Corrugated Tubes

Aamer Majeed Al-dabagh

Mechanical Engineering Department, University of Technology, Baghdad-Iraq
aamermajeed@yahoo.com

Falah Fakhir Hatem

Mechanical Engineering Department, University of Technology, Baghdad-Iraq

falahhatem59@yahoo.com

Ibrahim Emad Sadiq

Mechanical Engineering Department, University of Technology, Baghdad-Iraq

ibrahimemad1993@yahoo.com

Abstract

Three corrugated tubes with various corrugation depths are experimentally and numerically investigated. Air is used as a working fluid in tube side heated by saturated steam passing through the shell of heat exchanger where constant wall temperature at the tube side was achieved. The dimensionless corrugation depth (e/D_h) are 0.0216, 0.0469 and 0.0798. However, the corrugation angle (θ) and pitch to diameter ratio (p/D_h) were kept nearly constant of 9^o and 0.5, respectively. The experiments were carried out over the turbulent range of Reynolds number from 5000 to 50,000. The results reveal that the average Nusselt number is increased by 46%, 67% and 105% for corrugation depth ratios of 0.0216, 0.0469 and 0.0798, respectively compared with the smooth tube. However, the average friction factor of the corrugated tube with e/D_h = 0.0216, 0.0469 and 0.0798 are 90%, 135% and 500% higher than of smooth tube, respectively. At the same pumping power, the optimum Nusselt number ratio was 1.4 obtained by corrugated tube with intermediate depth ratio (e/D_h =0.0469). To visualize the Flow behavior of flow inside corrugated tubes, the numerical approach was used to solve three-dimensional governing equations with shear stress transport k-ω model by using ANSYS, Fluent 15. Solid work was used to generate the physical domain of corrugated tube. The numerical result showed that there is main vortex Generated in the main flow due to rotational flow induced along the helical path. In addition, secondary vortex is originated behind the rib. These two vortices can promote flow mixing between the flow layers and break the boundary layer. Consequently, achieve high heat transfer improvement.

Key words: Corrugated tube, Friction factor, Heat transfer, Performance evaluation criteria.

1. Introduction

Shell and tube heat exchanger are widely used in petrochemical industries, power plants, heating and cooling equipment and other. Several tube shapes and heat transfer enhancement technique have been introduced to improve the overall thermal-hydraulic performance of heat exchangers in order to reduce the heat exchanger size and the operational cost. One method of enhancing the tube convective heat transfer is to limit the growth of the thermal boundary layer associated with turbulent flow inside the tube. The thermal boundary layer can be made thinner or partially broken by flow disturbance. Disruption of the laminar sub layer in the turbulent boundary layer is an effective method for augmenting heat transfer. This disruption can be obtained by using micro-fin tube, coiled wire inserts, twisted tape insert, turbulator/ swirl generator devices [1]. These inserts are materials added to a tube which will impact on manufacturing cost and it will be more costly for corrosive gases and high temperature application. An alternative method to improve heat transfer enhancement is the surface modification which prompting earlier transition to turbulence, creating vortices that increase mixing or restarting the thermal boundary layer. The concept of using surface modification instead of inserting devices has gained attention since it has the combination of high heat transfer and a lower pressure loss penalty. Accordingly, many tube shapes have been proposed and used in shell and tube heat exchanger such as dimpled tube, corrugated tube, fluted tube, helical tube and elliptical axis tube. The studies have been reported extensively on the heat transfer and pressure drop characteristics in fluted and corrugated tubes for different parameters such as flow region, type of fluid, and shape of the fluted tube. [2] evaluated the heat transfer and pressure drop for fluid food and high viscous fluid Inside corrugated tubes. Beside augmented heat transfer rate, they also noted that corrugated tubes have an advantageous of easy to clean and decrease in fouling behavior in compare with other surface modification. Laminar flow of ethylene glycol in the entry region of corrugated tubes have been examined by [3]. It was discovered that the heat transfer does not significantly influence by the hydro-dynamically developing region. [4] reported the heat transfer and isothermal friction characteristics in corrugated tubes with different roughness geometries. It was found that the Nusselt number and friction factor coefficient of the corrugated tubes are higher than those of the smooth tube around 250% and 300%, respectively. [5] investigated the heat transfer and pressure drop in a corrugated tube for single-phase flow using ethylene glycol as the working fluid. The friction factor of corrugated tube was up to 2.45 times above the smooth tube. 18 helically corrugated tubes were experimentally carried out by [6]. It was studied the influence of corrugated pitch, corrugated height and corrugated angle on heat transfer augmentation. [7] examined experimentally the effects of pitch to diameter ratio and rib-height to diameter ratio of turbulent flow in helically corrugated tubes on thermal performance. It was reported that the pitch ratio was dominant only for the friction factor while the rib-height ratio was a key factor controlling the value of the Nusselt number and thermal performance factor characteristics. Non-isothermal friction factor and thermal performance criteria in tube side heat exchanger were also examined. They showed that the heat transfer and thermal performance of the corrugated tube was increased compared with those of smooth tube, subject to rib pitch/height ratio, and corrugated angle and Reynolds number. The results show an increase in friction factor within the range of 1.5 and 3.5 higher than that obtained for smooth tube. Isothermal friction factor and heat transfer of two three-start corrugated tubes combined with five twisted tapes inserts examined by [8]. The results show that the

tube side heat transfer coefficient was particularly high when corrugated tube was combined with a twisted tape. [9] investigated the heat transfer and friction factor of a discrete corrugated rib roughed tubes experimentally. The results showed that the maximum value of thermo-hydraulic performance was 1.95 corresponding to the corrugated tube with pitch to rib height ratio of 10 at the Reynolds number of 7343. [10], [11] and [12] were examined the heat transfer and friction factor of gas flow inside enhanced surface. [10] tested corrugated tubes at a relative lower ratio of corrugation pitch to corrugation height. [11] concentrated on a higher ratio. [12] tested cross corrugated and single corrugated tubes for exhaust gas numerically and experimentally. They increased the inlet temperature up to 450°C and employed water as cooling fluid (for gas cooling). They also examined the effect of tangential velocity existed along the helical ribs on friction and heat transfer.

The main target of this work is to further investigate the influence of corrugation depth on the performance of shell and tube heat exchanger with turbulent range of Reynolds number experimentally and numerically.

2. Tested Tubes

Corrugated tubes tested in this study were manufactured by cold forming. The deformations were achieved with a device containing one roller. Thus, one roller performs spirally corrugated tubes with one start per perimeter. The corrugated tubes tested in the current work are depicted in Figure 1. This figure also demonstrates the corrugation parameters of corrugated tube which characterized by corrugation pitch (p), corrugation depth (e) and the corrugation angle (θ). Whose corrugation angle depends on values of e, p and outer diameter (d_o) as follows [6]:

$$\theta = \tan^{-1}\left(\frac{P}{\pi(d_o - 2e)}\right) \quad (1)$$

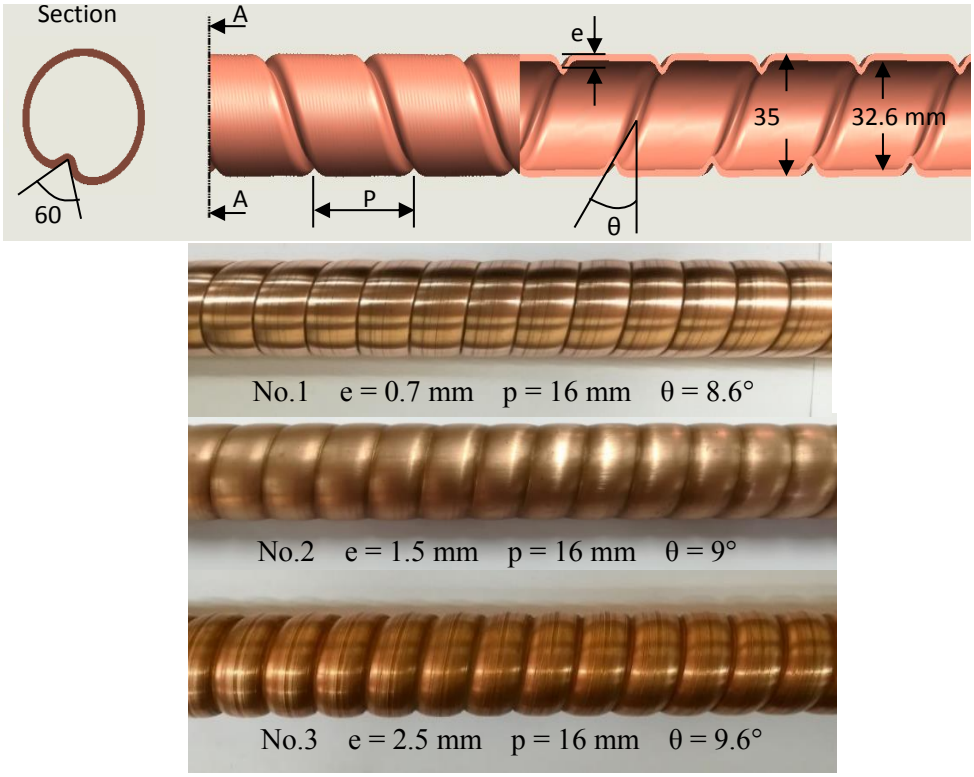

Figure 1: Photo of tested corrugated tubes and definition of corrugation parameters

Further details about dimensions of tested tubes are listed in Table 1. The corrugated tubes were made of the copper tubes with 32.6 mm inner diameter, 1.2 mm in thickness and 1600 mm in length, where the effective test length is 1250 mm.

Table 1: The dimensions of tested tubes: hydraulic diameter (D_h), corrugation pitch (p), corrugation depth (e), corrugation angle (θ).

NO.	D_h (mm)	e (mm)	P (mm)	e/D_h (-)	p/D_h (-)	p/e (-)	θ (°)
0	32.6	Smooth tube					
1	32.36	0.7	16	0.0216	0.494	22.85	8.6
2	31.93	1.5	16	0.0469	0.5	10.66	9
3	31.32	2.5	16	0.0798	0.51	6.4	9.6

3. Experimental Facility and Procedure

3.1 Experimental Set-up

Figure 2 and Figure 3 show the photo and the schematic diagram of the present experimental work. The test rig mainly comprises of a blower, air flow pipe, developing pipe, test section, exit section. The test section is shell and tube heat exchanger which consisted of two circular tubes; the inner tube of 35 mm in diameter made from copper is used as tested tube. The test tube is jacketed by tube of 76 mm in diameter. the jacket is sealed from both sides of the tube to achieve the require saturation steam temperature and pressure. The air flow rate through test section was measured by using orifice plate which manufactured according to British standard B.S 1042. Water U-tube manometer and micro-manometer were employed to measure pressure drop across orifice and test section, respectively. In order to evaluate the correct bulk fluid temperature at the exit of test section, a traverse mechanism was installed in the exit of test section as shown in Figure 4. The thermocouple and Pitot tube were connected with moving jaw of the traverse mechanism to measure the local temperature and local dynamic pressure distribution at the exit section. Consequently, the bulk fluid temperature can be evaluated. The pressure drop across test section was measured by two static pressure tapes located at the tube inlet and outlet. Also, the temperature in the inlet of test section was recorded.

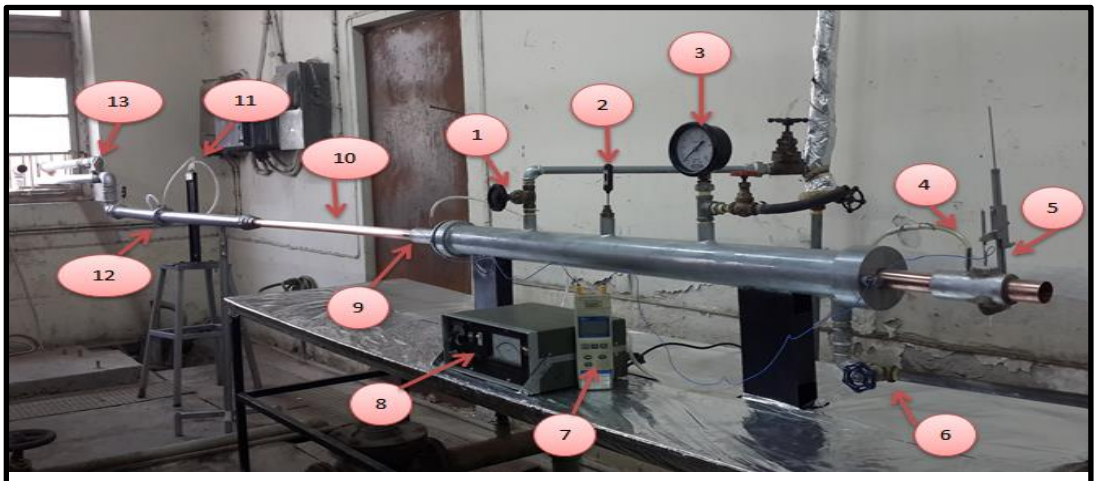

1-Steam valve. 2-Digital thermometer. 3-Bourdon gauge. 4-Pressure tapping. 5-Traverse mechanism. 6-Drain valve. 7-Thermocouple reader. 8-Micromanometer. 9-Coupling spool. 10-Developing pipe. 11-Water manometer. 12-Orifice plate. 13- Air control valves.

Figure 2: Photo of test rig

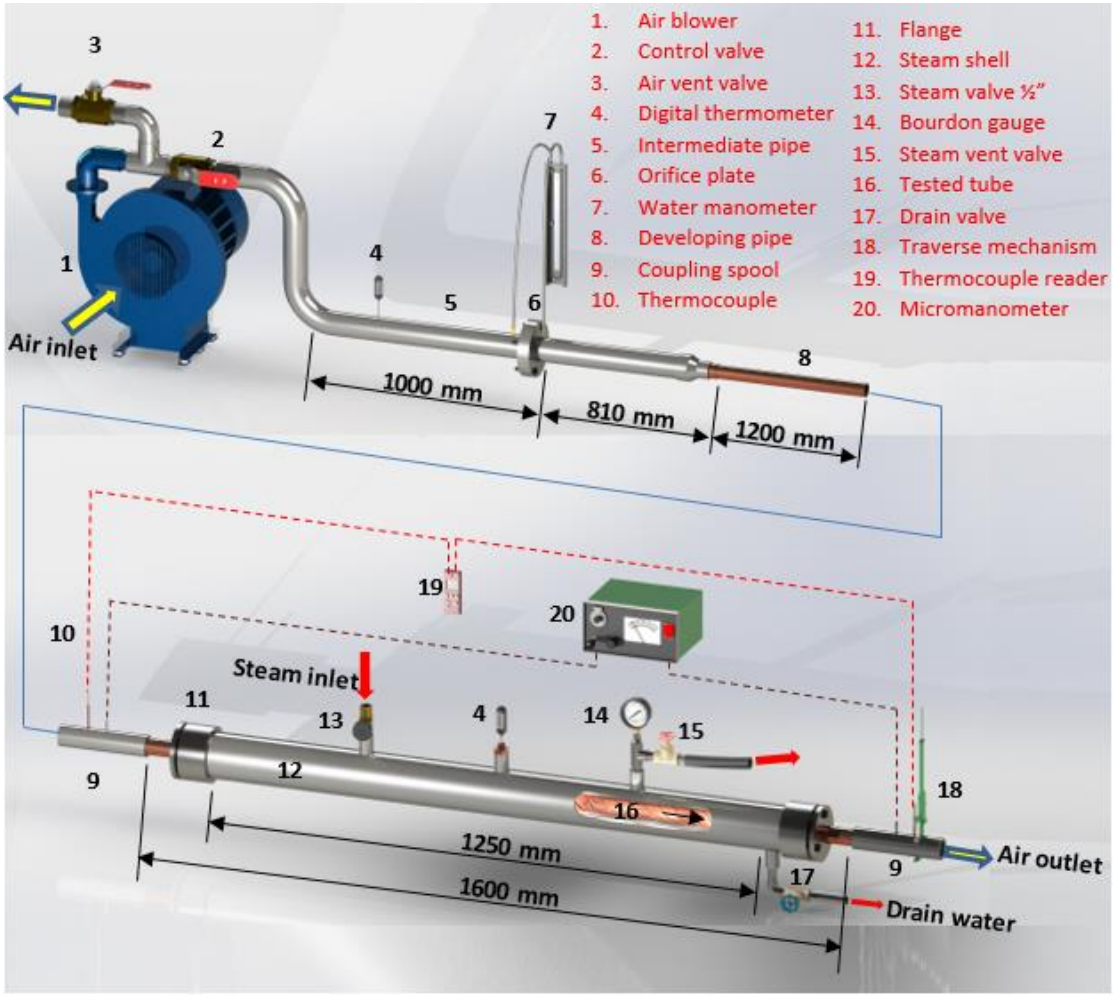

Figure 3: Schematic diagram of test rig

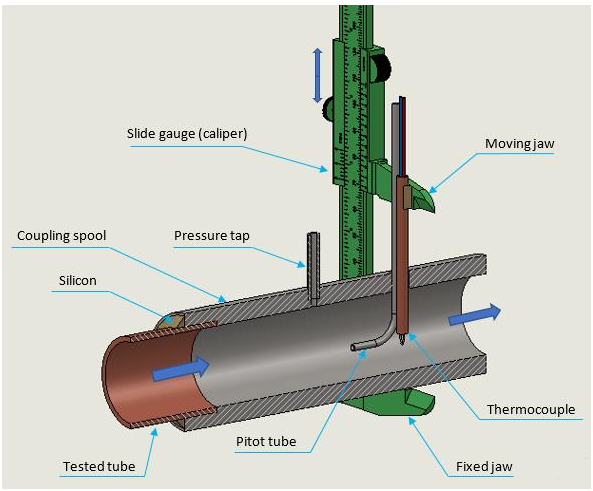

Figure 4: Traverse mechanism and the exit-coupling spool

3.2 Data Reduction

1- Heat transfer calculation:

A- Outlet air temperature ($T_{a\ out}$) calculation:

Due to heat transfer to the air stream, a thermal boundary layer will create along the flow, therefore temperature is varied in the flow radial direction. To evaluate the bulk fluid temperature at the outlet section, energy equation and perfect gas equation were combined, and the following equation was obtained.

$$T_{a\ out} = \frac{\int_0^R \sqrt{T(r)\,P_d(r)}\ \ r\ dr}{\int_0^R \sqrt{\frac{P_d(r)}{T(r)}}\ \ r\ dr} \quad (2)$$

Where, P_d = dynamic pressure = total pressure - static pressure … (3)

The outlet air temperature is calculated by using Simpson integration [13].

$$\int_0^R F(r)dr = \frac{step}{3}\left[F(r_o) + 2\sum_{j=1}^{n/n-2} F(r_{2j}) + 4\sum_{j=1}^{n/2} F(r_{2j}-1) + F(r_n)\right] \quad (4)$$

Step = 1 mm (traverse step along the radial direction measured by caliper)

B – Heat transfer coefficient calculation:

According to the first law of thermodynamic, for flow with constant specific heat, the heat transfer gained by the air can be estimated [14].

$$Q_a = \dot{m}_a\ Cp_a\ (T_{a\ out} - T_{a\ in}) \quad (5)$$

Where, $\dot{m}_a$ is air mass flow rate, Cp_a is air specific heat, $T_{a\ out}$ is outlet air temperature, $T_{a\ in}$ is inlet air temperature.

To express the convective heat transfer from the tube wall to the air, one can apply the newton's law of cooling [14].

$$Q_w = h_a\ A_w\ LMTD \quad (6)$$

Where, h_a is an air heat transfer coefficient, A_w is surface area, however LMTD denotes logarithmic mean temperature difference, it is estimated as follow [14]:

$$LMTD = \frac{(T_w - T_{a\ out}) - (T_w - T_{a\ in})}{Ln\left(\frac{T_w - T_{a\ out}}{T_w - T_{a\ in}}\right)} \quad (7)$$

According to conservation of energy (Q_w=Q_a), i.e. the heat gained by the air is the heat released by the tube wall. By combining equations (5) and (6), the convective heat transfer coefficient can be evaluated.

$$h_a = \frac{\dot{m}_a * cp_a * (T_{a\ out} - T_{a\ in})}{A_w * LMTD} \quad (8)$$

C- Nusselt number (Nu):

$$\mathrm{Nu} = \frac{h_a\, D_h}{k_a} \tag{9}$$

2- Friction factor (f) calculation:

The air friction factor can be estimated by measuring pressure drop through the test section.

$$\Delta p = \frac{G^2}{2\rho_{in}}\left[2\left(\frac{\rho_{in}}{\rho_{out}} - 1\right) + f\,\frac{L}{D_h}\rho_{in} v_m\right. \tag{10}$$

Where, $G = \frac{\dot{m}}{A_c}$ represents the fluid mass velocity and f in above equation means the Darcy-Weisbach friction factor. The mean specific volume v_m is calculated from:

$$v_m = \frac{1}{2}\left(\frac{1}{\rho_{in}} + \frac{1}{\rho_{out}}\right) \tag{11}$$

Equation (10) is obtained by applying Newton's second law of motion on differential element of test tube. Further detail about this equation is presented by [15]. The pressure drop analysis was done under non-isothermal condition. This was achieved because of the change of the fluid thermo-physical properties through the boundary layer due to temperature variation.

4. Numerical simulation

The numerical simulation or computational fluid dynamic CFD allows analysis of complicated flow characteristics without resort to a costly prototype for flow visualization with sophisticated experimental measurements. ANSYS, Fluent 15 software was used to simulate the complicated flow through the corrugated tubes.

4.1 Physical Geometry Description and Boundary Condition

Solid work software was used to generate the physical model of corrugated tube. The computational domain used in this study comprises of three sectors with a total length of 36 cm, as shown in Figure 5. The effective corrugated section has a length of 30 cm with 3 cm of plain tube connected at the upstream and downstream of the corrugated sector to eliminate the effect of disturbance in this region. In present investigation, one plain tube and three corrugated tubes were designed with same dimensions as those of tubes used in the experimental work.

The velocity distribution at the inlet is set as fully developed velocity boundary condition; this was achieved by implementing the developed equation 12 with Fluent using user defined function option. The inlet air temperature is set to be constant of 36 ^{o}C. The outlet condition is set as the pressure outlet boundary condition with a pressure of 0 KPa. No-slip wall conditions is adopted with constant wall temperature set to 115 ^{o}C.

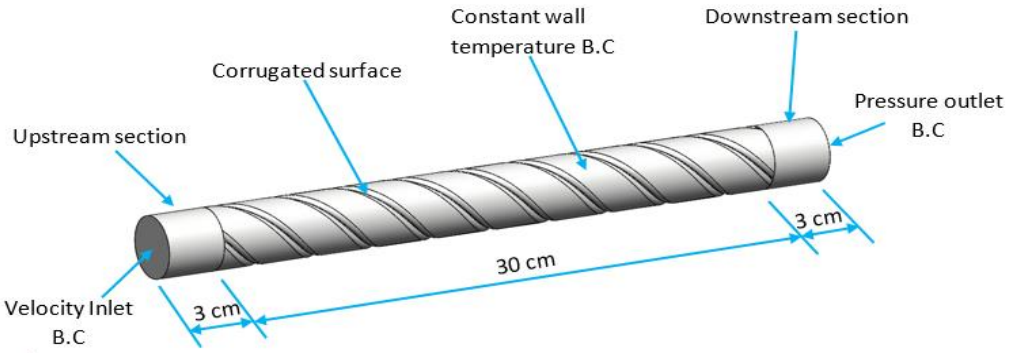

Figure 5: Computational domain and boundary condition

$$\frac{u}{u_{max}} = 0.1626\ ln\left(1 - \frac{r}{R}\right) + 1.0391 \qquad (12)$$

4.2 Mesh and Grid Independent Test

The flow field close to the surface is quite complex in corrugated tube, however this region has great impact on the friction factor and Nusselt number values. To achieve accurate flow prediction of flow characteristic, boundary layer mesh technique (prism mesh) is provided while tetrahedral mesh is employed for surface and body as shown in Figure 6.

To find the optimum mesh density for accurate solution with less possible time consumption, grid independent test is conducted. The grid independence test of corrugated tube is shown in Table 2**: Grid independence analysis**

. Four different mesh densities generated for corrugated tube. The results showed that the variation in Nusselt number and friction factor does not exceed 0.45% and 0.92%, respectively, when the number of mesh changes from 2,965,492 elements to 3,601,783 elements. The mentioned variation is small. So, to take the time consumption into consideration, mesh 3 was selected to solve this model.

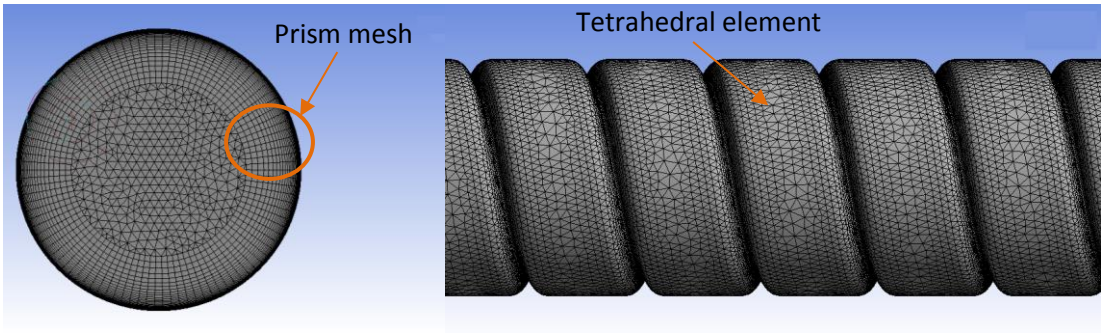

Figure 6: Mesh for the computational domain

Mesh	Number of elements	Nusselt number	Friction factor
Mesh 1	1998556	62.73	0.0896
Mesh 2	2488300	64.01	0.09171
Mesh 3	**2965492**	**64.8**	**0.09301**
Mesh 4	3601783	65.1	0.09388

Table 2: Grid independence analysis

4.3 Assumptions and Governing Equations

In the current simulation, the flow characteristics are assumed to be as Three-dimensional, steady state flow, constant thermal conductivity and specific heat, ideal gas flow, body force and dissipation term were neglected.

By taking the aforementioned assumptions into account, the governing equations characterizing the three-dimensional flow can be written as follow:

Conservation of mass:

$$\nabla \cdot \rho\vec{u} = 0 \quad (13)$$

Momentum equation:

$$\nabla \cdot (\rho\vec{u}\vec{u}) = -\nabla p + \nabla \cdot (\mu\nabla^2\vec{u}) \quad (14)$$

Energy equation:

$$\nabla \cdot \left(\rho\vec{u}c_p T\right) = \nabla \cdot (k\nabla T) \quad (15)$$

4.4 Chosen of Turbulence Model

Shear stress transport k-ω (*SST k-ω*) model has ability to predict the separation and reattachment better when compared to *k*-ε and the standard *k*-ω [16]. In the present work, the corrugated tube is predicted to generate a flow swirling and separation in the flow boundary layer, therefore the *SST k-ω* model is expected to be more appropriate in this case.

5. Results and Discussions

5.1 Heat Transfer

The presence of corrugation in tube normally induces flow disturbance and breaking of thermal boundary layer. consequently, increase the temperature difference between the surface temperature and the flow temperature close to it. Figure7 A shows the effect of three tubes of different corrugation depth ratios (e/D_h = 0.0216, 0.0469 and 0.0798) on heat transfer rate in term of Nusselt number. The results show that depth has a significant effect on the heat transfer, whereas the average Nusselt number is increased by 46%, 67% and 105% for corrugation depth ratios of 0.0216, 0.0469 and 0.0798, respectively compared with the smooth tube. The Nusselt number ratio (Nu/Nu_s) is shown in Figure7B. The results indicated that Nusselt number ratio is influenced by Reynolds number, where at lower value of Reynolds number, the enhancement ratio is strongly depending on the Reynolds number while at higher Reynolds number, the enhancement ratio becomes relatively independent. This is due to larger boundary layer thickness induced at low Reynolds number in smooth tube and implementing of corrugation in this region became more active on the flow mixing,

resulting in a sharp increase in Nusselt number ratio. While at higher Re, the boundary layer of smooth tube is thinner and the effect of flow separation and reattachment on the enhancement ratio at the wake region of the corrugated tube are relatively constant.

The reason behind the fact that Nusselt number increase with increase corrugation depth is related to the effect of secondary vortex that originate downstream of the ribs, as shown in Figure 7. The flow streamlines indicated that the vortex region and flow circulation are increasing with increase the corrugation depth. This is because of high adverse pressure induce at high corrugation depth. These recirculation regions between ribs play an important role to draw the core flow from the cold region to hot region and pushing the hot flow to the core region. Rotational flow streamlines of three tubes of different corrugation depths at cross section z = 300 mm and at Re = 5000 are demonstrated in Figure 8. The results reveal that the helical shape of the ribs creating rotational flow along the flow direction for different corrugation depth. In general, low rotational velocity induces at a region near the tube center, while the rotational velocity increases gradually in the region away from the tube center except the region very close to the tube surface, which have lower rotational velocity due to existing of velocity boundary layer. It is important to notice from Figure 8 that the rotational velocity increases with increase the corrugation depth. This is because at high corrugation depth, the high amount of flow rate adjacent to the ribs and follow the helical bath of the ribs resulting to increase the momentum of rotational flow in the entire flow. Both the secondary vortex generated behind the ribs and rotational flow (main vortex) generated due to the existing of the helical ribs affect on the temperature distribution and then flow mixing. Temperature contour of three tubes with different depths are presented in Figure 9. These results showed that when the corrugation depth increased, the cold region of core flow (the blue region in Figure 9) is decreased, which means that this core region of cold flow is mixed with the hot region of flow close to the surface resulting to increase the temperature difference between the wall and the flow close to it, thus a higher rate of heat transfer is achieved.

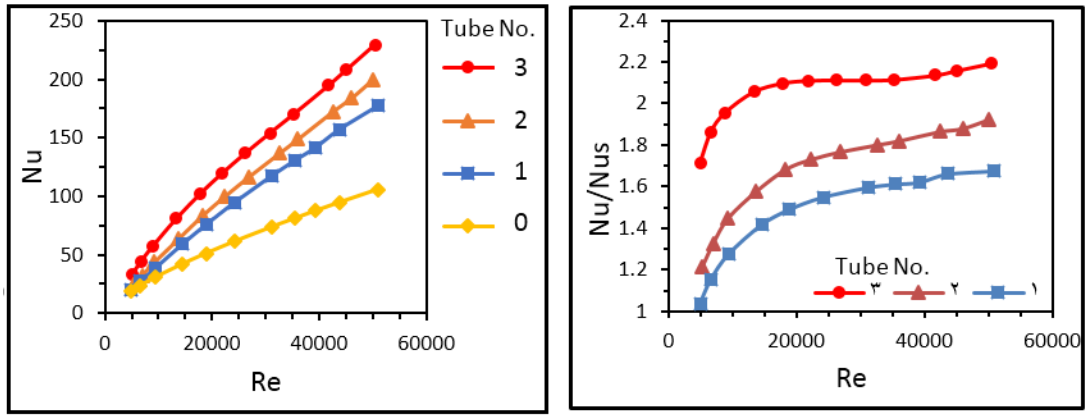

(A) Nusselt number vs Re (B) Nusselt number ratio vs Re

Figure 7: Nusselt number against Reynolds number for different depths

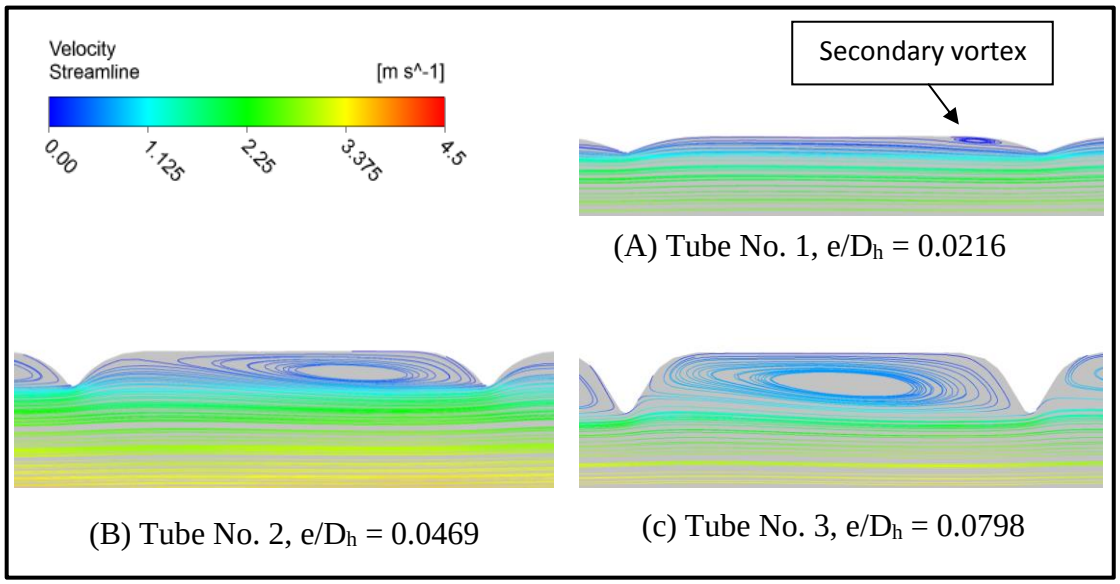

Figure 7: Velocity streamline for various depths at Re = 5000

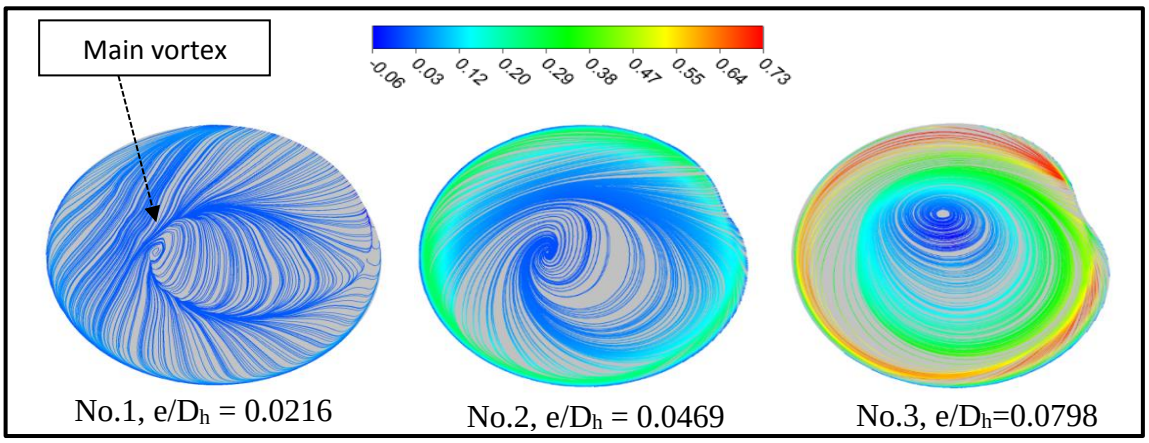

Figure 8: Rotational velocity streamline for different depths at Re = 5000

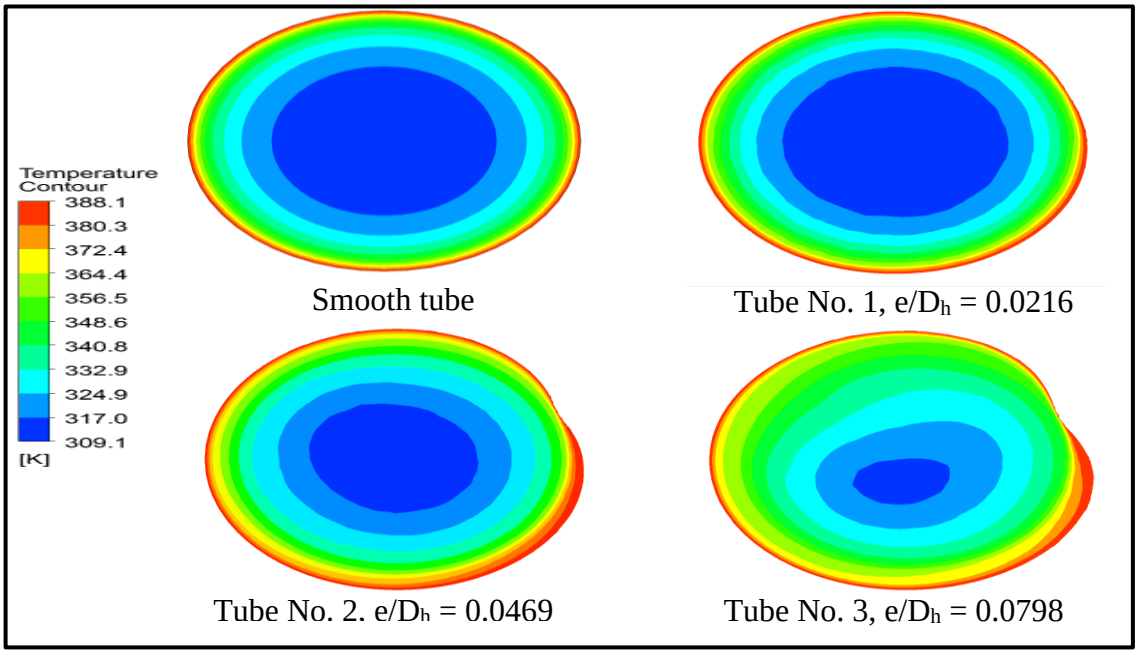

Figure 9: Temperature contour for corrugated tubes with different depths

5.2 Friction Factor

The flow inside corrugated tube is quite complicated. However, the pressure drop across the corrugated tube is caused by: (1) drag forces implemented on the fluid flow by the helical rib, (2) rotational flow generated by the helical rib, (3) frictional drag augmentation and (4), flow blockage related to reducing the cross-sectional area of tube. All these parameters would effect on the value of pressure drop and friction factor simultaneously, however, because the corrugated surface is an obstacle in the flow direction, the pressure drop due to drag is the main concern in this type of tube.

Figure 10A views the influence of corrugation depth ratio on the non-isothermal hydrodynamic losses of three different corrugation depths (e/D_h = 0.0216, 0.0469 and 0.0798). The non-isothermal hydrodynamic losses are exhibited in term of friction factor. In general, the trend of friction factor of corrugated tube is dissimilar to that of smooth tube. This is related to the effect of pressure drag as well as the effect of friction drag existed in corrugated tube, while in smooth tube, the only friction drag effects on the friction factor value, thus the trend of friction factor in corrugated tubes exhibit different behaviors. To evaluate the effect of the existing corrugated tubes with respect to the smooth tube, the friction factor ratio is presented in Figure 10.B. The results showed that the friction factor ratio is increasing significantly with increase Reynolds number for all corrugated tubes. The increasing in friction factor ratio with increase corrugation depth is significant at high Reynolds number. This is attributed to high rate of increase of pressure drag and rotational velocity with increase corrugation depth at high Reynolds number. At fix Reynolds number, the friction factor ratio is increasing with increase corrugation depth. This is because of the following reasons:

1- With increasing the corrugation depth, the secondary vortex region behind the rib is increased, see Figure 7, since this region induces high flow disturbance and high dissipation in flow energy.

2- The flow blockage is increasing with increase the corrugation depth, i.e. reducing the cross-sectional flow area, resulting higher flow velocity and then higher flow losses.

3- As the corrugation depth increased, the pressure gradient along the helical path of rib increased, resulting a large flow sweeping in the helical path which creates a high rotational flow as shown in Figure 8, this will lead to:

I- Increase the velocity gradient of flow close to the wall, leading to increase the shear stress between the flow and the wall, consequently, increase the drag due to friction.
II- Increase flow disturbance, this is because the rotational flow generates main vortex in the main flow, this vortex induces a high fluctuation in flow layers, hence high turbulence intensity.

These reasons make the friction factor increase with increase corrugated depth. Quantitatively, the mean friction factor of the corrugated tube with e/D_h = 0.0798, 0.0469 and 0.0216 are 500%, 135% and 90% higher than of smooth tube, respectively.

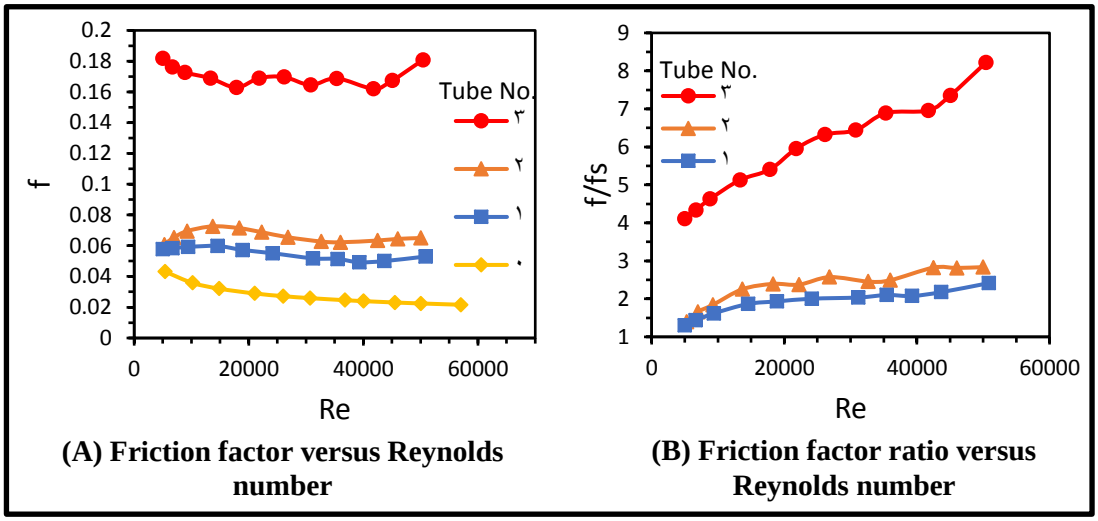

(A) Friction factor versus Reynolds number

(B) Friction factor ratio versus Reynolds number

Figure 10: Friction factor and friction factor ratio versus Reynolds number for various corrugation depth ratio

Figure 11 demonstrates the turbulence kinetic energy contour of corrugated tubes with three different corrugation depths. Physically, the turbulence kinetic energy is evaluated by measuring root mean square (RMS) velocity fluctuations which is produced by flow shear force, vortex generation and through exerting the force on the flow [17]. So, Turbulent Kinetic Energy (TKE) values can give an indication of the disturbance level in flow field. It is obvious from Figure 11 that the high TKE is produced from the tube with a higher corrugation depth, this is due to large secondary vortex generated behind the ribs, review Figure 7, and high rotational flow induced from tube with a high corrugation depth, review Figure 8, these flow patterns lead to increase the flow turbulence intensity. The maximum turbulence kinetic energy for tube with a corrugation depth ratio of 0.0216, 0.0469 and 0.0798 are 0.07 J/kg, 0.3 J/kg and 0.6 J/kg, respectively. Also, it can be noticed from Figure 11, for a certain corrugation depth ratio, the minimum TKE region is noticed at the core flow region of the tube which is the farthest region from roughness region, while the maximum value of TKE is observed at the location near the ribs. This was due to the high drag force exerted from the ribs on the flow, resulting a higher flow disturbance intensity in that region, but in region very close to the surface, TKE is decreased significantly due to viscosity effect. In addition, TKE continues to increase along the main flow direction. This fact is related to the accumulation of flow disturbance when the flow passes across the number of ribs along the corrugated tube. The similar basic pattern of the turbulence kinetic energy contours is obtained with different corrugation depth ratios, but the scale increases with increase the corrugation depth ratio.

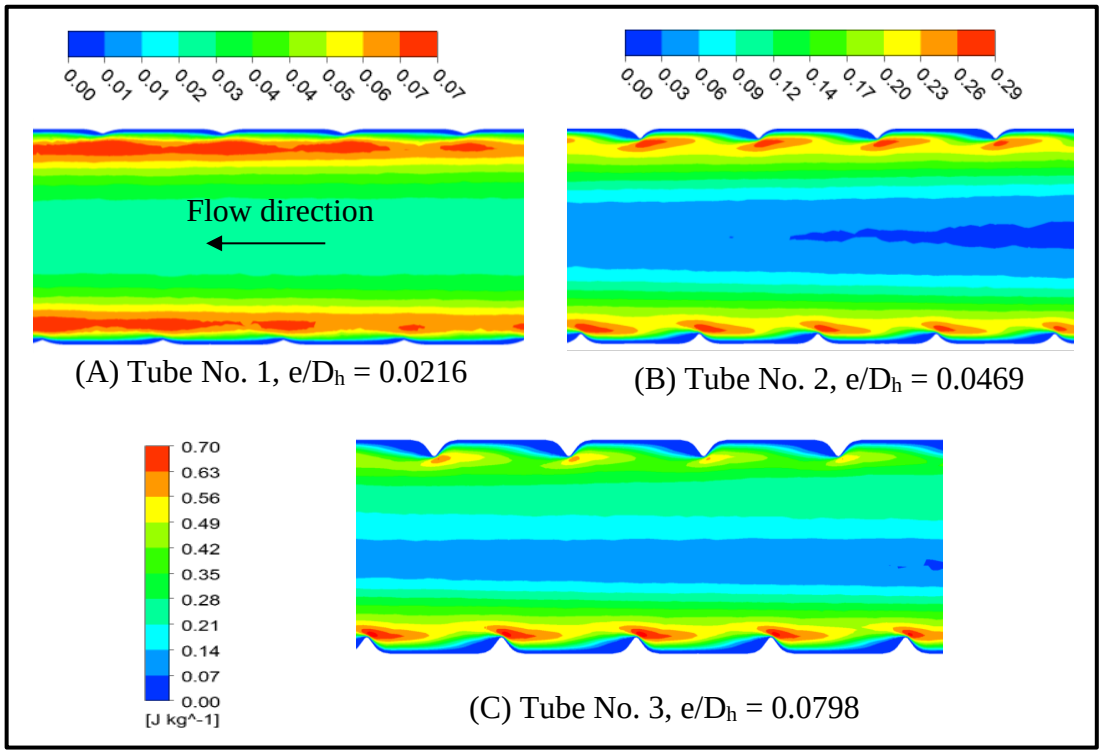

Figure 11: Turbulence kinetic energy contour for different corrugation depths

5.3 Performance Evaluation Criteria

To evaluate the performance of rough surfaces, [18] suggested the R3 criteria. This criterion characterizes the heat transfer augmentation of enhanced tube relatively to that of smooth tube at the fix pumping power in term of Nusselt number.

$$R3 = \frac{Nu}{Nu_s} \tag{16}$$

The limitation of fix pumping power is defined by:

$$Re_s = Re\left(\frac{f}{f_s}\right)^{\frac{1}{3}} \tag{17}$$

Figure 12 reveals the performance of tubes No. 1, 2, 3 (e/D_h = 0.0216, 0.0469, 0.0798). The tube with highest corrugation depth (e/D_h = 0.0798) achieves the best performance at lower Reynolds number value (Re = 5000-18000), while the tube with intermediate value of depth (e/D_h = 0.0469) provides better performance at higher value of Reynolds number (Re >18000). The enhanced tubes with e/D_h = 0.0798, 0.0469 and 0.0216 produce the maximum performances (R3) of 1.28, 1.4 and 1.32, respectively. This indicates that using the corrugated tube of e/D_h = 0.0469 and p/D_h = 0.5 can save 30 % of area at the same pumping power comparing with the smooth tube heat exchanger.

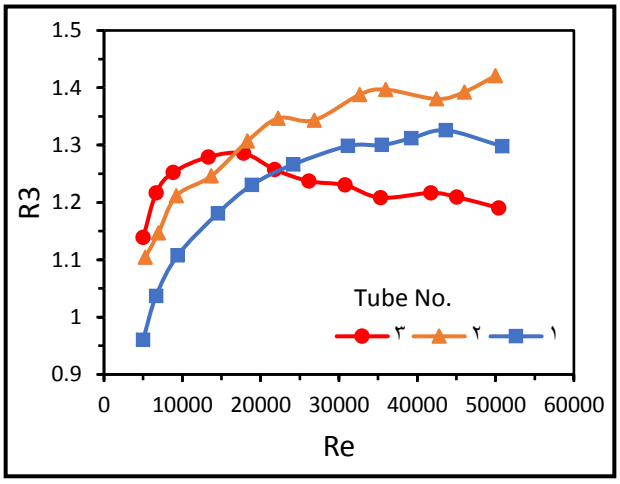

Figure 12: Performance against Reynolds number for three corrugated tubes with different depth ratios.

6. Conclusions

Three corrugated tubes with different corrugation geometries have been tested experimentally and numerically. Heat transfer enhancement, friction factor and performance of corrugated tube have been analyzed. The effects of the corrugation depth, corrugation pitch, corrugation angle and Reynolds number on thermo-hydraulic performance of the corrugated tube were studied. The result of this work can be outlined as follows:

- For all corrugated tubes the Nusselt number increases with an increase in Reynolds number, while friction factor decreases with increases Reynolds number for a wide range of Reynolds number. Higher value of friction factor and Nusselt number obtained by enhanced tubes in comparing with smooth tube based on the same condition.
- The Nusselt number and friction factor increases with increase in corrugation depth. Tube No. 3 with e/D_h = 0.0798, p/D_h = 0.51, θ = 9.6°, has highest average value of Nusselt number and friction factor of 2 and 6 times smooth tube, respectively.
- The highest value of the performance evaluation criteria (R3) is 1.4 corresponding to corrugated tube No.2 with e/d=0.0469, p/d= 0.5, θ = 9°, at Reynolds number of 50,000.

Nomenclature

A	Area	k	Thermal conductivity
A_c	Cross-sectional area	$\dot{m}$	Mass flow rate
Cp	Fluid specific heat	p	Corrugation pitch
d	Tube diameter	p_d	dynamic pressure
D_h	Hydraulic diameter	Q	Rate of heat transfer
e	Corrugation depth	R	Tube radius
f	Darcy-Weisbach friction factor	r	local radius
G	Fluid mass velocity	T	Temperature
h	Average heat transfer coefficient	u	Flow velocity component
v	Fluid specific volume		

Abbreviation

CFD	Computational fluid dynamics
FLUENT	Fluid and heat transfer software
LMTD	Logarithmic mean temperature difference
SST k-ω	Shear stress transport model

Greek symbols

θ	Corrugation angle
μ	Dynamic viscosity of fluid
ρ	Fluid density
Δp	Pressure drop

Subscript

a	Air
i	Horizontal direction
in	Inlet fluid
j	Vertical direction
m	Mean
max	Maximum
o	Outer side
out	Outlet fluid
s	Smooth tube
w	wall

Dimensionless numbers

Nu	Nusselt number
Re	Reynolds number

References

[1] Sheikholeslami M., Gorji-Bandpy M., and Ganji D. D., "Review of heat transfer enhancement methods: Focus on passive methods using swirl flow devices," *Renewable and Sustainable Energy Reviews,* vol. 49, pp. 444-469, 2015.

[2] Rozzi S., Massini R., Paciello G., Pagliarini G., Rainieri S., and Trifirò A., "Heat treatment of fluid foods in a shell and tube heat exchanger: Comparison between smooth and helically corrugated wall tubes," *Journal of Food Engineering,* vol. 79, pp. 249-254, 2007.

[3] Rainieri S. and Pagliarini G., "Convective heat transfer to temperature dependent property fluids in the entry region of corrugated tubes," *International Journal of Heat and Mass Transfer,* vol. 45, pp. 4525-4536, 2002.

[4] Vicente P. G., García A., and Viedma A., "Experimental investigation on heat transfer and frictional characteristics of spirally corrugated tubes in turbulent flow at different Prandtl numbers," *International Journal of Heat and Mass Transfer,* vol. 47, pp. 671-681, 2004.

[5] Barba A., Rainieri S., and Spiga M., "Heat transfer enhancement in a corrugated tube," *International Communications in Heat and Mass Transfer,* vol. 29, pp. 313-322, 2002.

[6] Harleß A., Franz E., and Breuer M., "Experimental investigation of heat transfer and friction characteristic of fully developed gas flow in single-start and three-start corrugated tubes," *International Journal of Heat and Mass Transfer,* vol. 103, pp. 538-547, 2016.

[7] Pethkool S., Eiamsa-ard S., Kwankaomeng S., and Promvonge P., "Turbulent heat transfer enhancement in a heat exchanger using helically corrugated tube," *International Communications in Heat and Mass Transfer,* vol. 38, pp. 340-347, 2011.

[8] Zimparov V., "Enhancement of heat transfer by a combination of three-start spirally corrugated tubes with a twisted tape," *International Journal of Heat and Mass Transfer,* vol. 44, pp. 551-574 , 2001.

[9] Kathait P. S. and Patil A. K., "Thermo-hydraulic performance of a heat exchanger tube with discrete corrugations," *Applied Thermal Engineering,* vol. 66, pp. 162-170, 2014.

[10] Esen E., Obot N., and Rabas T. J., "Enhancement: Part I. Heat transfer and pressure drop results for air flow through passages with spirally-shaped roughness," *Journal of Enhanced Heat Transfer,* vol. 1, 1994.

[11] Kidd G., "The heat transfer and pressure-drop characteristics of gas flow inside spirally corrugated tubes," *Journal of Heat Transfer,* vol. 92, pp. 513-518, 1970.

[12] Nelly S. M., Nieratschker W., Nadler M., Raab D., and Delgado A., "Experimental and Numerical Investigation of the Pressure Drop and Heat Transfer Coefficient in Corrugated Tubes," *Chemical Engineering & Technology*, vol. 38, pp. 2279-2290, 2015.

[13] Davis P. J. and Rabinowitz P., *Methods of numerical integration*: Courier Corporation, 2007.

[14] Cengel Y. A., *Heat tranfer a practical approach*: McGraw-Hill, 2003.

[15] Shah R. K.and Sekulic D. P. , 2003, *Fundamentals of heat exchanger design*: John Wiley & Sons.

[16] Menter F., "Zonal two equation kw turbulence models for aerodynamic flows," in *23rd fluid dynamics, plasmadynamics, and lasers conference*, p. 2906 , 1993.

[17] Pope S. B., "Turbulent flows," ed: IOP Publishing, 2001.

[18] Bergles A., Blumenkrantz A., and Taborek J., "Performance evaluation criteria for enhanced heat transfer surfaces," *Heat transfer,* vol. 2, pp. 239-243, 1974.

تأثير عمق النتوء على تحسين أنتقال الحرارة وخصائص الجريان للأنابيب المحلزنة

عامر مجيد الدباغ

قسم الهندسة الميكانيكية، جامعة التكنولوجيا، بغداد– العراق

aamermajeed@yahoo.com

فلاح فاخر حاتم

قسم الهندسة الميكانيكية، الجامعة التكنولوجية، بغداد– العراق

falahhatem59@yahoo.com

ابراهيم عماد صادق

قسم الهندسة الميكانيكية، الجامعة التكنولوجية، بغداد– العراق

ibrahimemad1993@yahoo.com

الخلاصة

تم أختبار ثلاثه انابيب محلزنه تحتوي على اعماق نتوء مختلفه عمليا ونظريا. الاختبار أنجز بامرار هواء بارد داخل الانبوب المحلزن، يسخن هذا الهوء بامرار بخار ماء مشبع داخل القشره المبادل الحراري هذا يؤدي الى جعل درجه حرارة سطح الانبوب تقريبا ثابته. قيم عمق النتوء الابعدي (e/D_h)هي 0.0216، 0.0469، 0.0798، بينما زاوية الحلزون ونسبه خطوه الحلزون (p/D_h) كانتا ثابتتان تقريبا 9^o و0.5، على التوالي. التجارب أنجزت على الهواء المضطرب حيث كان عدد رينولدزمن 5000 الى 50000. النتائج أظهرت ان معدل الزيادة في عدد نسلت كانت 46%،67% و105% لنسبة عمق نتوء 0.0216، 0.0469 و0.0798، على التوالي بالمقارنه مع الانبوب الاملس. بينما، معدل الزيادة لمعامل الاحتكاك للانابيب الملتويه ذات نسبة عمق التواء 0.0216، 0.0469 و0.0798 كانت 90%، 135% و500% اعلى من الانبوب الاملس، على التوالي. بثبوت قدرة دافعة الهواء فان أفضل نسبة عدد نسلت كانت 1.4 التي تم الحصول عليها من انبوب محلزن يحتوي على نسبة عمق نتوء متوسط القيمة (e/D_h= 0.0469). أستخدم الحل العددي لتصور تصرف الجريان داخل الانبوب المحلزن بأستخدام برنامج Ansys, Fluent 15. النتائج النظريه اظهرت ان هنالك دوامة رئيسيه تتكون نتيجه حركه المائع بمسار حلزوني، بالاضافه الى ذلك هنالك دوامة اخرى تتكون خلف النتوء. هذان الدوامتان تقومان بعملية خلط بين طبقات المائع وكذلك تكيسر طبقه المتاخمه، وبالنتيجة يؤدي الى تحسين انتقال الحرارة.

الكلمات المفتاحيه: أنبوب محلزن، معامل أحتكاك، انتقال الحراره ومعيار تقييم الاداء.